Vortex phase transitions in monolayer FeSe film on $SrTiO_3$

2016 2D Mater. 3 024006

(http://iopscience.iop.org/2053-1583/3/2/024006)

2D Materials

CrossMark

RECEIVED
7 December 2015

REVISED
14 February 2016

ACCEPTED FOR PUBLICATION
25 February 2016

PUBLISHED
28 April 2016

PAPER

Vortex phase transitions in monolayer FeSe film on $SrTiO_3$

Weiwei Zhao[1], **Cui-Zu Chang**[2], **Xiaoxiang Xi**[1], **Kin Fai Mak**[1] **and Jagadeesh S Moodera**[2]

[1] The Center for Nanoscale Science and Department of Physics, The Pennsylvania State University, University Park, PA 16802-6300, USA
[2] Francis Bitter Magnet Lab and Department of Physics, Massachusetts Institute of Technology, Cambridge, MA 02139, USA

E-mail: wzhao@phys.psu.edu and czchang@mit.edu

Keywords: 1UC FeSe/$SrTiO_3$, 2D superconductor, vortex phase transition

Supplementary material for this article is available online

Abstract

The voltage–current (*V*–*I*) characteristics in superconducting monolayer FeSe film on $SrTiO_3$ (100) under different magnetic fields are investigated. The zero-field *V*–*I* result exhibits signatures of a Berezinski–Kosterlitz–Thouless transition, a characteristic of two-dimensional (2D) superconductors. Under an applied magnetic field, with current density lower than the critical current density, the sheet resistance versus current density (R_{sq}–*J*) dependence changes from ohmic (R_{sq} independent of *J*) to non-ohmic (a nonlinear dependence of R_{sq} on *J*) as the temperature decreases, indicative of a vortex phase transition/crossover. We interpret the high-temperature phase as the vortex liquid phase and the low-temperature phase as the vortex slush phase, which has short-ranged vortex lattice correlation, while long-range correlation (i.e. true superconductivity) is absent. No transition into a vortex glass phase is seen, illustrating the importance of thermal fluctuations in a perfect 2D superconductor under a magnetic field.

Introduction

The vortex phase transition is one of the most fascinating research topics in the physics of type-II superconductors under a finite magnetic field. The existence of a vortex liquid–glass transition, which separates a high-temperature vortex liquid (VL) phase from a low-temperature vortex glass (VG) phase [1–3], has been demonstrated in many three-dimensional (3D) superconductors such as cuprates [4–8], MgB_2 [9], Nb [10, 11] and W [12]. In the VG phase, a true superconducting state with zero resistance exists due to pinning of the vortices. On the other hand, a nonzero but exponentially small resistance remains in the VL phase. In the two-dimensional (2D) limit, due to the significantly enhanced thermal fluctuation effects, only the VL phase is present at finite temperatures. The absence of a VL–VG transition at finite temperatures in 2D superconductors has been theoretically predicted and experimentally verified in 2D superconducting films [13, 14].

In this paper, we report experimental evidence of a different vortex phase transition in a recently discovered high-temperature 2D superconductor, a monolayer of FeSe on $SrTiO_3$ [15–21]. Instead of a VL–VG transition, as the temperature decreases a transition/crossover from a VL phase to a vortex slush (VS) phase is revealed by examining the voltage–current (*V*–*I*) dependence. The VS phase is characterized by a short-range vortex lattice correlation without a long-range correlation. The presence of finite resistance (although exponentially small at low temperatures) makes it distinctively different from the zero-resistance VG phase. While both of the VL–VS and VS–VG transitions have been observed in bulk $YBa_2Cu_3O_7$ single crystals [22], no VS–VG transition is observed in monolayer FeSe/$SrTiO_3$ films, potentially due to the strongly enhanced thermal fluctuation effects in 2D superconductors.

Materials and method

The FeSe films studied here were grown using a custom-built ultrahigh vacuum molecular beam epitaxy (MBE) system. The insulating $SrTiO_3$ (100) substrates with a specific TiO_2-terminated surface were prepared using standard chemical and thermal treatments in a tube furnace. Then, the $SrTiO_3$ substrates were transferred into the MBE chamber and annealed at 600 °C for 1 h before FeSe film growth. FeSe films were grown at a rate of approximately 0.2

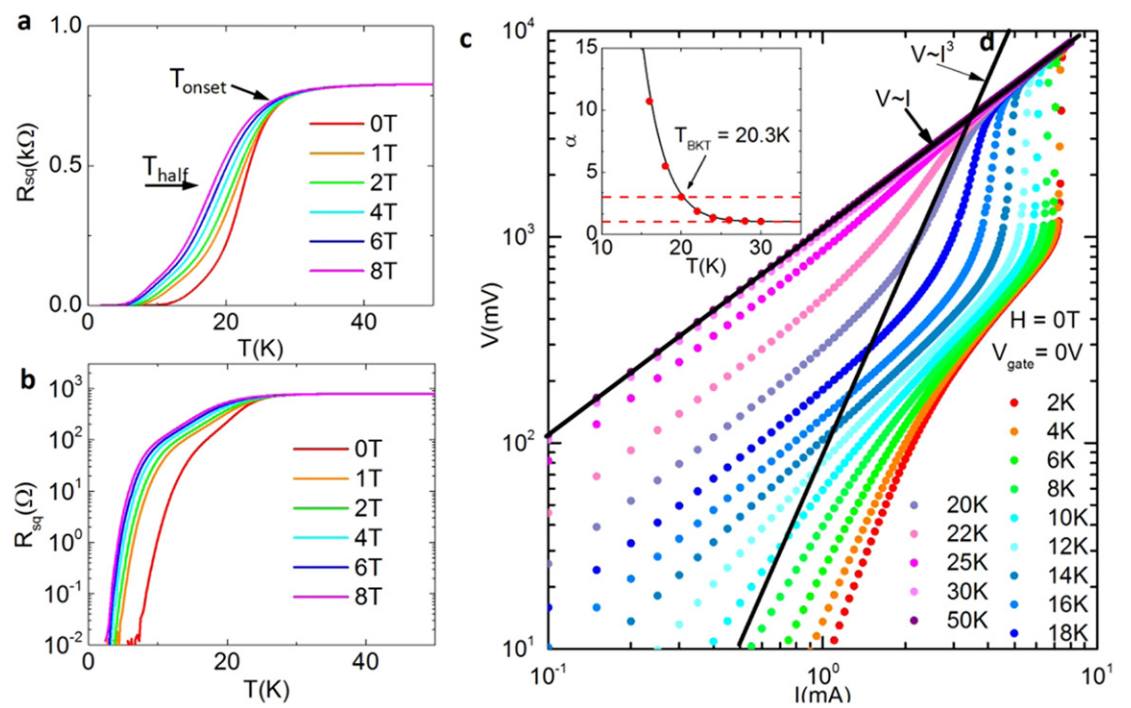

Figure 1. (a) R_{sq} in a linear–linear scale as function of T under different H in the range 0 to 8 T. (b) R_{sq} in log scale as a function of T under different H in the range 0 to 8 T. (c) $V–I$ isotherms from 2 K to 50 K plotted on a log–log scale. The two black solid lines correspond to $V–I$ and $V–I^3$ dependences, respectively. The inset shows the exponent α as a function of T, deduced from the power-law fittings, and yields $T_{BKT} = 20.3$ K when $\alpha = 3$.

layers/min on the $SrTiO_3$ substrate by coevaporating Fe(99.995%) from an e-gun source and Se(99.999%) from a Knudsen cell with a flux ratio of 1:10 at 330 °C. A post-grown annealing of the film at 550 °C for 2 h was needed to make FeSe films superconducting. Then, additional 10 unit cell FeTe was deposited on the FeSe film as a capping layer to prevent its atmosphere exposure, similar to a previous method for *ex situ* transport measurement [20]. Transport measurements were performed by using a standard six terminal hall-bar geometry with a width of 0.89 mm and length of 1.25 mm between the two voltage electrodes.

Results and discussion

The sheet resistances (R_{sq}) as a function of temperature (T) were measured with $I = 500$ nA for the 1UC FeSe/$SrTiO_3$ with 10UC FeTe capping layers. As shown in figures 1(a) and (b), R_{sq} is 790 Ω when $T = 50$ K and starts dropping from ~30 K to lower than <0.04 Ω when T_{zero} is ~7 K, below the measurement sensitivity. The superconducting transitions become broader and shift to lower temperatures with increasing H, which are typical characteristics of superconducting transition in thin films. It is natural to attribute the broader transitions of $R_{sq}(T)$ in our 1UC FeSe superconducting layer to the Berezinski–Kosterlitz–Thouless (BKT) phase transition. Strong support for BKT physics is found in the zero-field $V–I$ isotherms measured over a range of different T. As shown in figure 1(c), the measured $V–I$ curves exhibit I^{α} power-law dependence, and is precisely what is expected for a system governed by the BKT mechanism [23–26]. In the BKT scenario, the excitation current breaks apart the bound vortex–anti-vortex pairs and give the sample a non-ohmic behavior with increasing current. At higher currents, the rate of increase of V with I is reduced and the $I–V$ curves revert toward ohmic. There are free vortices above the BKT transition temperature, $T_{BKT,}$ and bound vortex–anti-vortex pairs lower energy than the free vortex below T_{BKT}. In the region where V shows the most rapid increase with I, it varies as I^{α} with a temperature dependent exponent $\alpha(T)$. The exponent α increases gradually from 1 as the temperature decreases and crosses 3 at T_{BKT}, which we assign as the BKT transition temperature ($T_{BKT} = 20.3$ K as shown in the inset of figure 1(c)). Contrary to the theoretical prediction of a sharp jump from 1 to 3 at T_{BKT}, the gradual change of α is likely caused by disorder effects in our monolayer sample, which smears out the sharp transition.

Below, we describe the $R_{sq}–J$ characteristics under perpendicular H, which is numerically computed from the $V–I$ data under H. The $R_{sq}–J$ isotherm at various T from 2 to 50 K at $H = 1$ T is shown in figure 2(a). At the critical current density J_c, R_{sq} shows an abrupt jump to a normal state value, indicating that the superconductivity is completely destroyed above J_c. J_c is found to shift to lower values with increasing T, exhibiting a typical superconducting behavior.

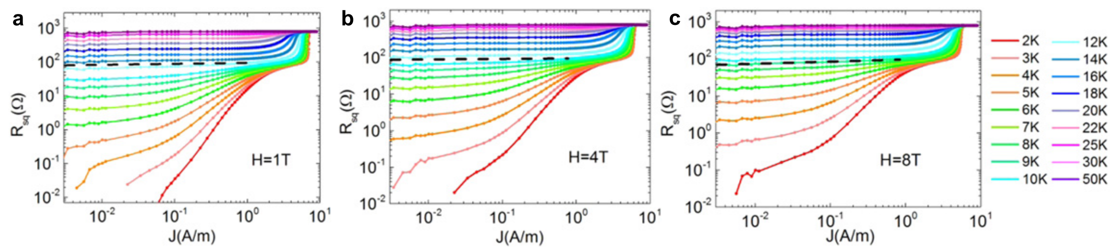

Figure 2. R_{sq}–J isotherms from 2 K to 50 K under perpendicular $H = 1$ T (a), 4 T (b), 8 T (c). The black dashed lines reprent the transition from ohmic to nonlinear behavior at T^*. T^* as function of H is plotted in figure 3.

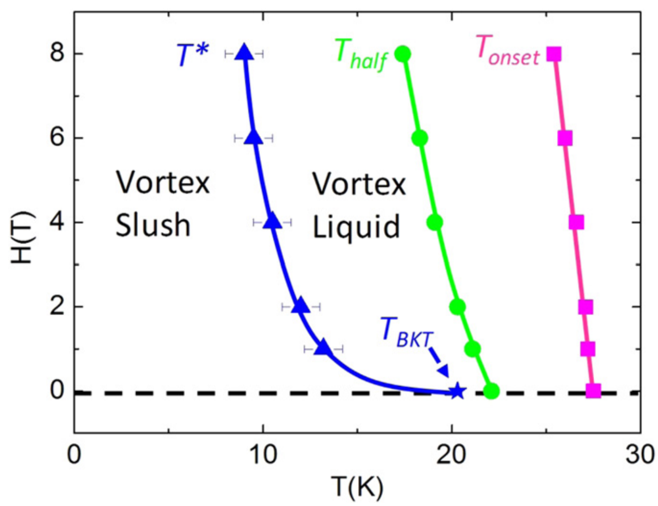

Figure 3. Vortex melting phase diagram including the boundery curves of T^*, T_{half} and T_{onset} as a function of H. $T^*(H)$ is the vortex lattice melting transition temperature between the VL and VS phases at fixed H determined from figure S1. T_{KTB} is the BKT transition temperature at $H = 0$ determined from figure 1. T_{onset} and T_{half} are defined as the temperature at which the resistance is 90% and 50% of the normal resistance at 50 K, respectively.

With J well below J_c, however, R_{sq}–J dependence exhibits two different regimes depending on T, indicative of two phases: (I) when the temperature T is just below the superconducting transition temperature, R_{sq} shows ohmic behaviors (independent of J) until $T = \sim 13$ K at which R_{sq} is nearly an order of magnitude lower than the normal state sheet resistance; (II) when T goes lower than ~ 13 K, R_{sq} starts dropping with nonlinear 'S sharp'. R_{sq} drops rapidly first when J goes below J_c and then drops slowly when J goes further below ~ 0.1 A m^{-1} and saturates to a very small nonzero value when $J \rightarrow 0$, although the value can be much smaller than those in phase I. We did not take -measurements below 2 K due to the limits of the equipment. Here we define the temperature at which the R_{sq}–J characteristics cross from linear dependence of phase I to nonlinear dependence of phase II as T^*. T^* in the case of $H = 1$ T is ~ 13 K as shown by the black dashed line in figure 2(a). T^* are ~ 10 K and ~ 9 K at $H = 4$ T (figure 2(b)) and $H = 8$ T (figure 2(c)), respectively. According to a previous study [12], the transition temperature for the VG–VL transition can be identified by first plotting the slope (dV/dI) as a function of I for each T. The maximum value of dV/dI is identified, and T^* is determined at the maximum rate of change of $(dV/dI)^{-1}$ with respect to T. We have used the same method to identify T^*, and have shown procedures in figure S1 in the supplementary materials. We found that the T^* values are 13.2 K, 9.2 K, 8.0 K for $H = 1$ T, 4 T, 8 T, respectively, consistent with the identification in figure 2.

The boundary curve of T^* as function of H is plotted in figure 3, which separates the high-temperature phase I and the low-temperature phase II. Phase I exhibits the typical ohmic characteristics of the VL phase observed in previous experiments. Phase II, which is different from either the VL or VG phase, was not observed in previous experiments for thin films and constitutes the key new result of our work. The R_{sq}–J dependence goes downward nonlinear when J is well below J_c, indicating that the current assisted vortex flow as current increases, and excitations emerge that destroy the short-range correlations. But R_{sq} as $J \rightarrow 0$ is still finite, suggesting long-range correlations are absent, i.e. phase II is not a true VG phase. Consequently, phase II exhibits the typical characteristics of a VS phase observed in defect-enhanced

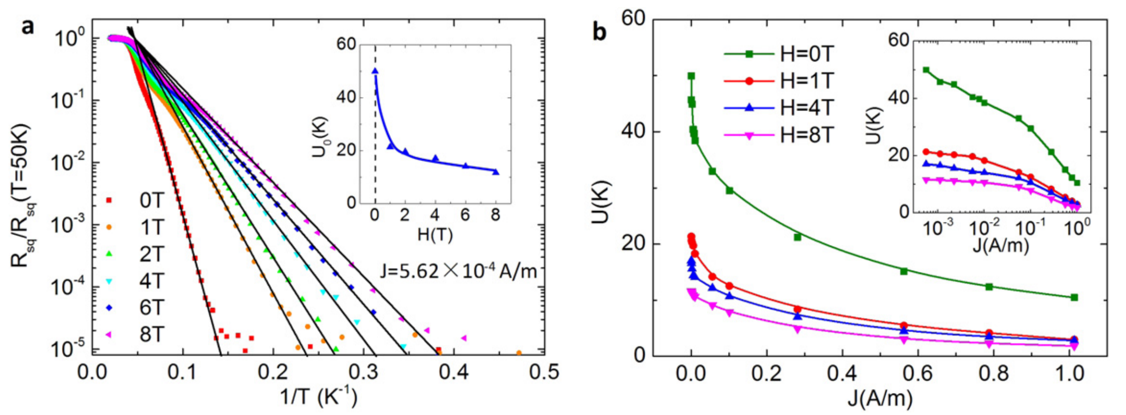

Figure 4. The activation energy of the thermally activated flux flow (TAFF). (a) The lnR_{sq} versus $1/T$ plot for the experimental data in figure 1(a). Black solid lines are the fitting lines deduced by equation (1). The activation energy U for TAFF for different H can be obtained by the fitting slope, as shown in the inset. (b) U as function of J under different fixed H. The inset is the same plot with J in the log scale.

$YBa_2Cu_3O_7$ single crystals by radiation damage [22]. The authors argued that an optimal disorder density is the critical factor to see this VS phase with only short-range vortex lattice correlation. We believe the 2D thermal fluctuation effect of our monolayer FeSe film grown on $SrTiO_3$ is important for the absence of long-range vortex lattice correlations. We also notice that T^* decreases with increasing H but the slope dT^*/dH becomes less steep with increasing H, as shown in figure 3. This feature is quite similar to the phase diagram observed for the melting of a flux-line solid in anisotropic layered materials such as BSCCO, for which $T_{melting}$ is almost independent of H in a high-field regime [27]. When the external field is high enough, interaction between adjacent pancake vortices in the same layer is stronger than the interaction between those in adjacent layers but on the same vortex line, causing the quasi-2D character for BSCCO.

Now we move on to extracting the energy barrier U, which depends on H and J, for vortex flows. In the region of a thermally activated vortex flow (TAVF), lnR_{sq} versus $1/T$ can be described by

$$R_{sq}(H, J) = R_0 \exp[-U(H, J)/T] \quad (1)$$

where R_0 is a temperature independent constant and $U(H, J)$ is the activation energy of the flux flow dependent on H and J. As shown in figure 4(a), the experimental data in figure 1(a) with $J = 5.62 \times 10^{-4}$ A m^{-1} or $I = 500$ nA exhibit kinks in the lnR_{sq} versus $1/T$ plots close to $T^*(H)$, suggesting the TAVF activation energy is different below and above T^*. The lnR_{sq} versus $1/T$ curves at different H are linear in the region below T^* and can be well fitted by equation (1) (black solid lines). The fitting lines obtained from lnR_{sq} versus $1/T$ at different H can be well extrapolated to meet at the same temperature, $T^{**} = 21$ K, which is close to T_{KTB}. In addition, the activation energy $U(H)$ for $J = 5.62 \times 10^{-4}$ A m^{-1} can be obtained by the fitting slope. As shown in the inset of figure 4(a), U quickly decreases once H is turned on. We have also compared our data to a logarithmic and a power-law dependence as shown in figure S3 of the supplementary materials, but none of them reproduces our data perfectly. As U not only depends on H but also on J, the J dependence of U under fixed H has also been studied, as shown in figure 4(b). U increases rapidly with decreasing J, but U increases slowly and saturates at a finite value after J is lower than ~0.1 A m^{-1} (see the inset of figure 4(b)). The J dependence of U can be understood as short-range excitations emerging as J increases, which effectively lower the activation energy for vortex flow. In addition, U saturates to a finite value when $J \rightarrow 0$ indicates the presence of TAVF, consistent with a finite resistance state in the $J \rightarrow 0$ limit shown in figure 2. For a true VG phase, U should diverge when $J \rightarrow 0$. Our observation doesn't match this description due to the presence of the finite U in the $J \rightarrow 0$ limit, further confirming that phase II is not a true VG phase, but a VS phase with short-range correlation.

According to the VG transition theory, the V–I curves at different T near the transition temperature can be scaled into two branches by the scaling equation. It is noted that the 2D VG theory has also been developed, and verified in some cases of extremely thin superconducting films [13, 14]. Interestingly our data cannot achieve a scaling collapse for any combination of the fitting parameters by using either a 3D or 2D scaling equation. The failure is not surprising because the transition/crossover observed in this paper is in fact a transition/crossover between VL and VS instead of a VL–VG transition. It is still unknown whether a true VG phase can occur when T goes to much lower temperatures below 2 K. Future experiments, especially study of V-I characteristics down to mK for this system, are needed.

Conclusion

To conclude, we observed an unexpected vortex slush phase in a monolayer FeSe film on $SrTiO_3$. The phase is characterized by a short-range vortex lattice correlation while the long-range correlation is absent. The presence of a finite resistance in the $J \rightarrow 0$ limit makes it distinctively different from the zero-resistance vortex glass phase. Thermal fluctuations in a perfect 2D superconductor under a magnetic field is the reason that no transition to the true vortex glass phase is seen in the monolayer $FeSe/SrTiO_3$ film.

Acknowledgment

We thank Moses H W Chan for fruitful discussions. This work was funded by the Penn State MRSEC, Center for Nanoscale Science, under award NSF DMR-1420620. KFM acknowledges support from the US Department of Energy, Office of Basic Energy Sciences under contract DESC0013883. Work at MIT is supported by the grants NSF DMR-1207469 and ONR N00014-13-1-0301, and the STC Center for Integrated Quantum Materials under NSF grant DMR-1231319.

References

[1] Fisher M P A 1989 Vortex-glass superconductivity—a possible new phase in bulk high-Tc oxides *Phys. Rev. Lett.* **62** 1415–8
[2] Fisher D S, Fisher M P A and Huse D A 1991 Thermal fluctuations, quenched disorder, phase-transitions, and transport in type-II superconductors *Phys. Rev.* B **43** 130–59
[3] Nattermann T and Scheidl S 2000 Vortex-glass phases in type-II superconductors *Adv. Phys.* **49** 607–704
[4] Koch R H, Foglietti V, Gallagher W J, Koren G, Gupta A and Fisher M P A 1989 Experimental-evidence for vortex-glass superconductivity in Y-Ba-Cu-O *Phys. Rev. Lett.* **63** 1511–4
[5] Jiang W, Yeh N C, Reed D S, Kriplani U, Tombrello T A, Rice A P and Holtzberg F 1993 Vortex-solid melting and depinning in superconducting Y-Ba-Cu-O single-crystals irradiated by 3-MEV protons *Phys. Rev.* B **47** 8308–11
[6] Zhang Y Z, Deltour R, de Marneffe J F, Wen H H, Qin Y L, Dong C, Li L and Zhao Z X 2000 Vortex characteristics in a superconducting Bi_2Sr_2-xLaxCuO6+delta thin film *Phys. Rev.* B **62** 11373–6
[7] Taylor B J, Li S, Maple M B and Maley M P 2003 Vortex-melting and vortex-glass transitions in a high purity twinned $YBa_2Cu_3O_7$-delta single crystal *Phys. Rev.* B **68** 9
[8] Xu H, Li S, Anlage S M, Lobb C J, Sullivan M C, Segawa K and Ando Y 2009 universal critical behavior in single crystals and films of $YBa_2Cu_3O_7$-delta *Phys. Rev.* B **80** 104518
[9] Yang H, Jia Y, Shan L, Zhang Y Z, Wen H H, Zhuang C G, Liu Z K, Li Q, Cui Y and Xi X X 2007 I-V characteristics of the vortex state in MgB_2 thin films *Phys. Rev.* B **76** 6
[10] Villegas J E, Gonzalez E M, Sefrioui Z, Santamaria J and Vicent J L 2005 Vortex phases in superconducting Nb thin films with periodic pinning *Phys. Rev.* B **72** 6
[11] Villegas J E and Vicent J L 2005 Vortex-glass transitions in low-Tc superconducting Nb thin films and Nb/Cu superlattices *Phys. Rev.* B **71** 7
[12] Sun Y, Wang J, Zhao W W, Tian M L, Singh M and Chan M H W 2013 Voltage-current properties of superconducting amorphous tungsten nanostrips *Scientific Reports* **3** 7
[13] Dekker C, Woltgens P J M, Koch R H, Hussey B W and Gupta A 1992 Absence of a finite-temperature vortex-glass phase-transition in 2-deensional $YBa_2Cu_3O_7$-delta films *Phys. Rev. Lett.* **69** 2717–20
[14] Woltgens P J M, Dekker C, Koch R H, Hussey B W and Gupta A 1995 Finite-size effects on the vortex-glass transition in thin $YBa_2Cu_3O_7$-delta films *Phys. Rev.* B **52** 4536–44
[15] Wang Q Y *et al* 2012 Interface-induced high-temperature superconductivity in single unit-cell FeSe films on $SrTiO_3$ *Chin. Phys. Lett.* **29** 4
[16] He S L *et al* 2013 Phase diagram and electronic indication of high-temperature superconductivity at 65 K in single-layer FeSe films *Nat. Mater.* **12** 605–10
[17] Tan S Y *et al* 2013 Interface-induced superconductivity and strain-dependent spin density waves in $FeSe/SrTiO_3$ thin films *Nat. Mater.* **12** 634–40
[18] Lee J J *et al* 2014 Interfacial mode coupling as the origin of the enhancement of Tc in FeSe films on $SrTiO_3$ *Nature* **515** 245–U207
[19] Sun Y, Zhang W H, Xing Y, Li F S, Zhao Y F, Xia Z C, Wang L L, Ma X C, Xue Q K and Wang J 2014 High temperature superconducting FeSe films on $SrTiO_3$ substrates *Scientific Reports* **4** 8
[20] Zhang W H *et al* 2014 Direct observation of high-temperature superconductivity in one-unit-cell FeSe films *Chin. Phys. Lett.* **31** 5
[21] Ge J F, Liu Z L, Liu C H, Gao C L, Qian D, Xue Q K, Liu Y and Jia J F 2015 Superconductivity above 100 K in single-layer FeSe films on doped $SrTiO_3$ *Nat. Mater.* **14** 285–9
[22] Worthington T K, Fisher M P A, Huse D A, Toner J, Marwick A D, Zabel T, Feild C A and Holtzberg F 1992 Observation of separate vortex-melting and vortex-glass transitions in defect-enhanced $YBa_2Cu_3O_7$ single-crstals *Phys. Rev.* B **46** 11854–61
[23] Epstein K, Goldman A M and Kadin A M 1981 Vortex-antivortex pair dissociation in two-dimensional superconductors *Phys. Rev. Lett.* **47** 534–7
[24] Hebard A F and Fiory A T 1983 Criticle-exponent measurements of a two-dimensional superconductor *Phys. Rev. Lett.* **50** 1603–6
[25] Kadin A M, Epstein K and Goldman A M 1983 Renormalization and the Kosterlitz-Thouless transition in a two-dimensional superconductor *Phys. Rev.* B **27** 6691–702
[26] Zhao W *et al* 2013 Evidence for Berezinskii-Kosterlitz-Thouless transition in atomically flat two-dimensional Pb superconducting films *Solid State Commun.* **165** 59–63
[27] Tinkham M 1975 *Introduction to Superconductivity* (New York: McGraw-Hill Inc.)